Available online at www.sciencedirect.com
SCIENCE DIRECT
Polymer 46 (2005) 11489–11498
polymer
www.elsevier.com/locate/polymer

# Processing and characterization of epoxy nanocomposites reinforced by cup-stacked carbon nanotubes

Young-Kuk Choi [a,*], Yasuo Gotoh [b], Koh-ichi Sugimoto [a], Sung-Moo Song [a], Takashi Yanagisawa [c], Morinobu Endo [a]

[a] *Faculty of Engineering, Shinshu University, 4-17-1 Wakasato, Nagano-shi, Nagano 380-8553, Japan*
[b] *Faculty of Textile Science and Technology, Shinshu University, 3-15-1 Tokida, Ueda-shi, Nagano 386-8567, Japan*
[c] *GSI Creos Corporation, minami watarida-chou, 1-12 Kawasaki-ku, Kawasaki-shi, Kanagawa 210-0855, Japan*

Received 14 June 2005; received in revised form 18 September 2005; accepted 6 October 2005
Available online 25 October 2005

**Abstract**

The effect of the dispersion, ozone treatment and concentration of cup-stacked carbon nanotubes on mechanical, electrical and thermal properties of the epoxy/CSCNT nanocomposites were investigated. Ozone treatment of carbon fibers was found to increase the surface oxygen concentration, thereby causing the contact angle between water, epoxy resin and carbon fiber to be decreased. Thus, the tensile strength, modulus and the coefficient friction of carbon fiber reinforced epoxy resin were improved. Moreover, the dispersion of fibers in polymer was increased and the electrical resistivity was decreased with the addition of filler content. The dynamic mechanical behavior of the nanocomposite sheets was studied. The storage modulus of the polymer was increased by the incorporation of CSCNTs. But the glass transition temperature decreased with increasing fiber loading for the ozone treated fiber composites. The ozone treatment did affect the morphology, mechanical and physical properties of the CSCNT.


*Keywords:* Nanocomposite; Polymer; Cup-stacked carbon nanotubes

## 1. Introduction

Carbon nanotubes (CNTs) have demonstrated remarkable high potential of mechanical and physical properties due to their structure, size and topology [1–6] that make them attractive for use in various applications especially as nanotube reinforced materials in nanocomposites, nanoelectronic devices, etc. [7–10]. However, the processing of such systems still need optimization in order to obtain uniform dispersion, controlled interfacial properties, and eventually orientation in a composite. There are two types of carbon nanotubes i.e. single-walled carbon nanotubes which have one graphene layer and multi-walled carbon nanotubes which have many graphene layers rapping onto themselves. They can be produced using various production methods such as arc-discharge [11,12], laser ablation [13], solar energy. By these methods, the carbon nanotubes are produced often with impurities and are difficult to produce in large-scale amounts at low cost. In recent years with the increasing understanding of carbon nanotubes properties, it is possible to produce high amounts of the nanotubes with high purity at low price using a catalytic chemical vapor deposition (CCVD) method, especially by a floating reactant method [14–21].

In this research work, we used the new type of carbon nanotubes obtained by a floating reactant method with a large hollow core and a large portion of open edges at the outer surface and also in the inner channels [22,23]. The main features of this carbon nanotubes consist of truncated conical graphene layers, called cups-stacked carbon nanotubes (CSCNTs). Due to their specific structural characteristics, physical and mechanical properties and their potentially low cost of much larger quantity production are interesting for their possible applications, principally such as reinforcement in nanocomposite materials [24–28]. Therefore, polymer composites are the main application of CSCNTs. For application of the CSCNTs as reinforcing fiber, the fibers must be homogeneously dispersed in polymer matrices. The fibers also must possess a good functional groups of the outer surface to make a low contact angle and high surface energies. This creates a strong interface interaction between the polymers

* Corresponding author. Tel.: +81 26 269 5670; fax: +81 26 269 5109.
*E-mail address:* choi_young_kuk@yahoo.fr (Y.-K. Choi).

0032-3861/$ - see front matter © 2005 Elsevier Ltd. All rights reserved.
doi:10.1016/j.polymer.2005.10.028

and the fillers so as to affect efficient load transfer from the polymer to the fibers.

There are various common surface treatments of carbon fibers in previous works that involve oxidation, whereby oxygen-containing as functional groups are formed on the surface of the fibers. We can achieve the oxidation by heat treatment in air, oxygen, chemical treatment [29], plasma treatment [28] and ozone treatment [30–32] etc. Therefore, these functionalizations are possible to achieve a good interface between CSCNTs and the polymer matrix and to obtain polymer/CSCNT nanocomposites with good properties.

In this work, we treated the CSCNT by ozone because the ozone treatment increases the bond strength of interface between fiber and matrix [33]. This result is very interesting for motivating us to investigate the effect of ozone treatment on properties of the fiber reinforced polymer composite. Therefore, uniform dispersion within the polymer matrices and improved CSCNT/matrix wettability and adhesiveness are important issues for CNTs in the processing of nanocomposites. Some researchers also obtained well dispersed CNTs in a polymer by high energy sonication of polymer solution containing dispersed CNTs followed by a solution–evaporation method, which successfully achieved homogeneous composites [34–36].

This article deals with the preparation of the CSCNT/epoxy nanocomposites by the in situ process using before and after ozone treated fibers. The fiber properties addressed are the wettability by water and the epoxy matrix, surface composition and morphology. And the nanocomposite properties addressed are the influences of the dispersion state of fiber in the polymer and the analysis of the mechanical (tensile strength, modulus and friction), electrical (volume electrical resistivity) and thermal properties of nanocomposite sheets. The effect of ozone treatment and untreatment on the fiber morphology and on the properties of nanocomposites was evaluated by the SEM and TEM observations.

## 2. Experimental procedure

### 2.1. Materials

For this study, cup-stacked carbon nanotubes (CSCNTs) used in this experiment are produced by GSI Creos Corporation, Japan, with the diameter and length as 60–100 nm and 20–40 μm, respectively. This nanofiber was produced by a floating reactant method using ferrocene or iron pentacarbonyl such as a catalyst precursor, hydrogen sulfide as a co-catalyst, and natural gas as a carbon feedstock in a continuous process [23,37,38]. Heat treatment of the tubes was carried-out to 1000–1200 °C. Recently, kilogram quantities are available from the manufacturer. A scanning electron microscopy (SEM) image of these fibers is showed in Fig. 1. They are highly entangled and relatively long and straight shape carbon nanofibers. But there are probably some catalyst particles amorphous carbon and onions as impurities.

Prior to the dispersion processing in an epoxy matrix, the fibers were dried at 120 °C in a vacuum for 24 h to remove adsorbed water, and then a sieve was used at 106 and 53 μm in order to reduce the size of aggregation of CSCNT and large impurities.

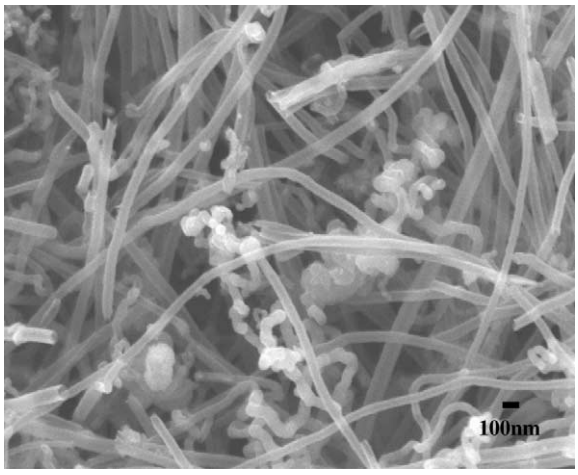


Fig. 1. FE-SEM images of as-produced cup-stacked carbon nanotubes.

The polymer matrix was prepared by mixing 20 parts by volume of epoxy resin based bisphenol A resin, supplied from Japan Epoxy Resin Co. Ltd. with 1.5 parts of triethylenetetramine as a hardner.

### 2.2. Ozone treatment

Cup-stacked carbon nanotubes surface were treated with ozone in a reactor and loaded CSCNTs surface were treated with ozone in a reactor and loaded with 1 g of carbon fiber under a constant ozone flow of 1 l $min^{-1}$. Ozone was produced from $O_2$ in ozone generator (OZSD-300A, Ebara-Jitsugyo Co. Japan) and the ozone concentration of the $O_3/O_2$ mixture was 36 g $m^{-2}$.

The CSCNT was put in the reactor and oxidized with ozone by flowing the ozone/oxygen mixture at room temperature through the reactor. The surface treatments included immersion with stirring 400 rpm of the fibers at room temperature for 1 h.

After ozone treatment, treated fibers were filtered and then dried at 100 °C in the muffle furnace for 12 h.

### 2.3. Preparation of CSCNT/epoxy nanocomposite sheets

The nanocomposites were made of epoxy and CSCNTs by a solution–evaporation method with presser processing. Two types of nanocomposites were made: epoxy + CSCNT untreated and CSCNT ozone treated.

To prepare the sample, the CSCNTs were dispersed in acetone by sonification and the stirring process at room temperature, 600 rpm for 15 min. The epoxy resin was poured into the CSCNT–acetone solution then sonification and stirring processes continued in order to disperse the fiber into the epoxy matrix at the ambient temperature, 600 rpm for another 15 min. In order to evaporate the acetone, the mixtures were placed in the muffle furnace at 100 °C for 24 h. After complete

evaporation of acetone, the mixture was placed in a vacuum oven to remove the voids at 80 °C for 30 min and then the hardener was blended into the mixtures at room temperature for 10 min. Next, the mixture was put again in a vacuum oven to remove the voids at room temperature for 10 min. When the mixture reached the gel state, a small amount of mixture was placed between two metal plates and compressed to try to reduce the residual voids. The plates were compressed with a uniform thickness between 0.12 and 0.17 mm. The nanocomposite sheets were prepared with contents of 0, 5, 10 and 20 wt% of CSCNT. Subsequently, the samples were then post-cured at room temperature for 16 h followed by 120 °C for 3 h to completely cure the materials.

Values for voids content were determined using the ASTM D2734 test method A. Void content measures the voids in reinforced polymers and composites. This void content information is very useful to estimate the composites strength.

To measure the voids, after the actual density of the material is determined the weighed sample is placed into a weighed crucible and burned in a 600 °C muffle furnace in air until only the reinforcing material remains. The crucible is cooled and weighed. The resin content can be calculated as a weight percent from the available data. We calculated the voids content, a five specimens were measured and averaged for each measurement.

### 2.4. Surface characterizations

To understand the surfaces wettability of CSCNT, the contact angles of pure water and epoxy resin before curing were measured. The sessile drop method at room temperature was used for these measurements as well as the powder method with the same bulk density.

The surface chemical composition of the samples was also determined by X-ray photoelectron spectroscopy (XPS).

XPS spectra were obtained with a VG ESCALAB photoelectron spectrometer using monochromatic Al Kα radiation (1486 eV), spot size of ca. 400 μm, the source being operated at 15 kV and 100 W. The vacuum in the analysis chamber was maintained at $10^{-8}$ Pa.

### 2.5. Volume electrical resistivity

Volume electrical resistivity measurements were taken by the standard four-point technique. The volume electrical resistivity, $\rho_v$ was calculated using the following equation:

$$\rho_v = \frac{R\mathrm{A}}{L} \tag{1}$$

where $R$ is the electric resistance, $A$ is the area of electrode and $L$ is the distance between electrodes. The square shape specimens for electric measurement had 10 mm on the side

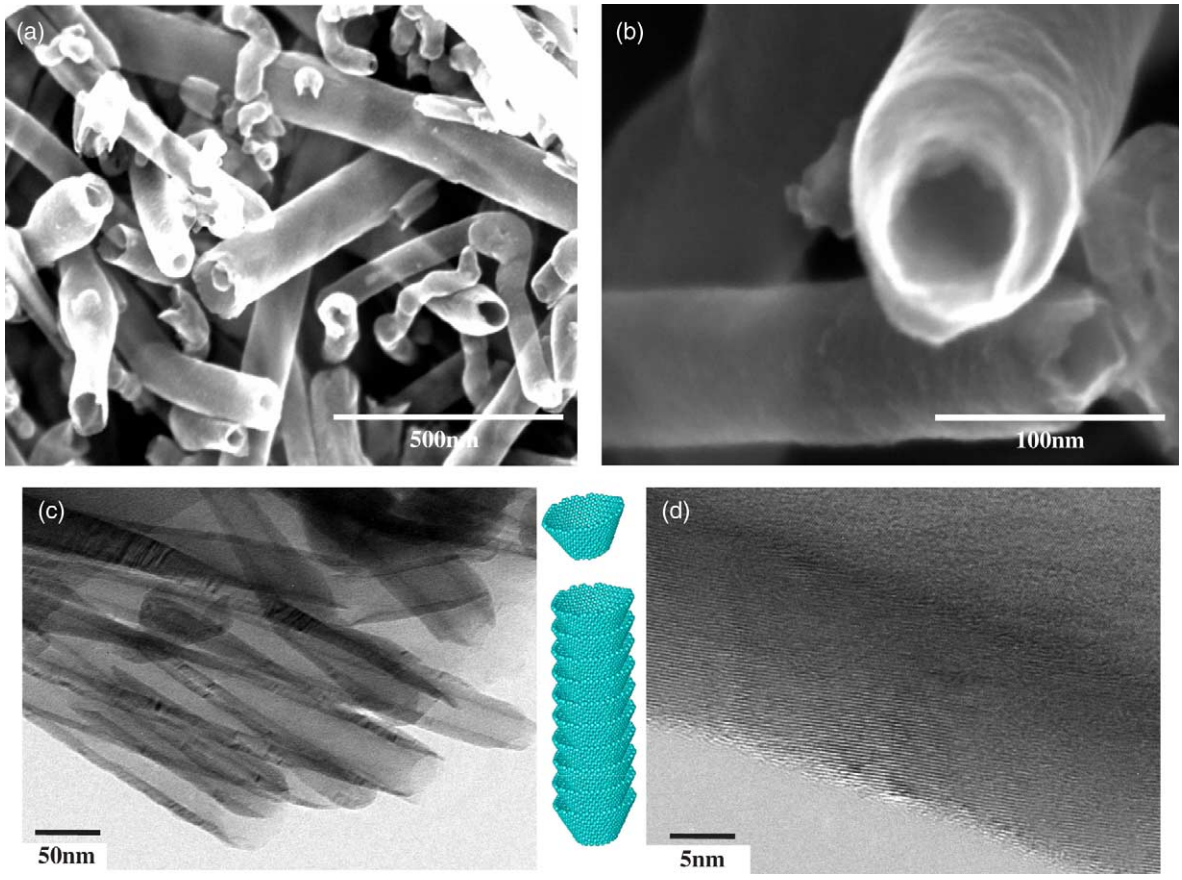


Fig. 2. (a) and (b) Low and high resolution FE-SEM images of CSCNT, showing a opening of tubes tip; (c) and (d) low and high resolution TEM images of CSCNT, showing the hollow core along the tube length and graphene layers.

and thickness of 0.12–0.17 mm. Before electric measurement, the surfaces were mechanically polished to remove the epoxy resin and minimize the influence of the porosity.

### 2.6. Mechanical tests

The tensile strength and Young's modulus were obtained by Shimadzu tensile tester (AGS-J). All tests were conducted at the ambient temperature and at a cross-head speed of 1 mm $min^{-1}$. The sample strips for tensile test were prepared with suitable dimensions and the gauge length was 5 mm.

The friction coefficient was obtained from friction test which was performed by sliding of a pin on a sample disc at 25 °C and 40% relative humidity. Before each test, the surface of counterpart pin was abraded with No. 1200 abrasive paper and cleaned with alcohol-dipped cotton, followed by drying. This friction test consisted of a rectangular nanocomposite pin sliding against nanocomposite sheets. The sliding speed of friction test was set at 0.1, 1 and 3 mm $s^{-1}$ under a constant load of 10 N during 20 cycles. Another friction test was also performed at sliding velocity of 0.5 mm $s^{-1}$ and the various loads used were 1, 5 and 10 N during 50 cycles. Then the friction coefficient was measured.

### 2.7. Thermal analysis

To examine the thermal properties of the matrix, dynamic mechanical thermal analyzer (DMTA) measurements were performed on nanocomposite sheets at all concentrations of CSCNT. The storage ($E'$) and loss modulus ($\tan\delta$) were obtained by DMTA using the ITK DVA-225 instrument in a stretching mode of frequency of 10 Hz. DMTA test samples were 20 mm × 4 mm × 0.12–0.17 mm and the samples were heated from room temperature to 200 °C at a heating rate of 5 °C $min^{-1}$. Glass transition temperature ($T_g$) was defined as the tan $\delta$ peak temperature.

### 2.8. Surface topography

Field emission scanning electron microscopy (FE-SEM) images obtained from SEM S-4100. Nanocomposite samples were sputter coated with Pt for 90 s Hitachi E-1030 coater. TEM micrographs were taken on a JEOL JEM-2010 FEF instrument to observe the structural of the CSCNT.

## 3. Results and discussion

### 3.1. Morphology of CSCNTs and nanocomposite sheets

FE-SEM and TEM images of as-received CSCNT are shown in Fig. 2. In this figure, SEM images of the fiber at low and high resolutions are shown in Fig. 2(a) and (b), respectively. They exhibit that the CSCNT fiber has a straight hollow tube structure, the open ends and various diameters. TEM images are represented in Fig. 2(c) and (d). The TEM images also shows the main characteristics of CSCNT with large hollow cores and some difference in the ration of the outer diameter to the inner diameter. In particular, the low-resolution TEM image clearly reveals the truncated conical graphene layers showing the cup-stacking morphology as represented with an illustration.

Fig. 3(a) and (b) shows SEM images of as-received and ozone treated CSCNTs, respectively. The surface morphologies of the fibers are likely unchanged by ozone treatment. However, after the treatment, the surface became slightly rougher than without the treatment.

To evaluate the dispersion state of the CSCNTs in the epoxy matrix, Fig. 4 shows the SEM images of fractured cross section of the composites containing untreated and treated CSCNTs (5 and 20 wt%). SEM measurement was observed for fractured cross section obtained by tensile test of the composites. At the first glance, the fractured cross section of every composite exhibits a good dispersion state of CSCNT, and there seems to be no difference in the dispersion state between untreated and treated CSCNTs. Occasional voids are particularly observed in the epoxy matrix when the fillers content is 20 wt% (Fig. 4(b) and (d)), which

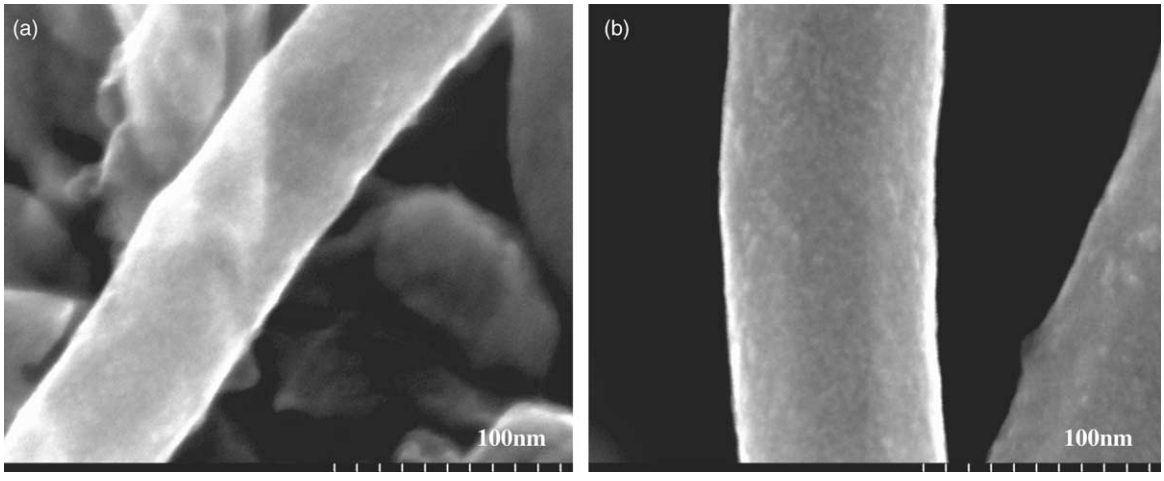


Fig. 3. SEM photographs of CSCNT surfaces (a) untreated; (b) ozone treated.

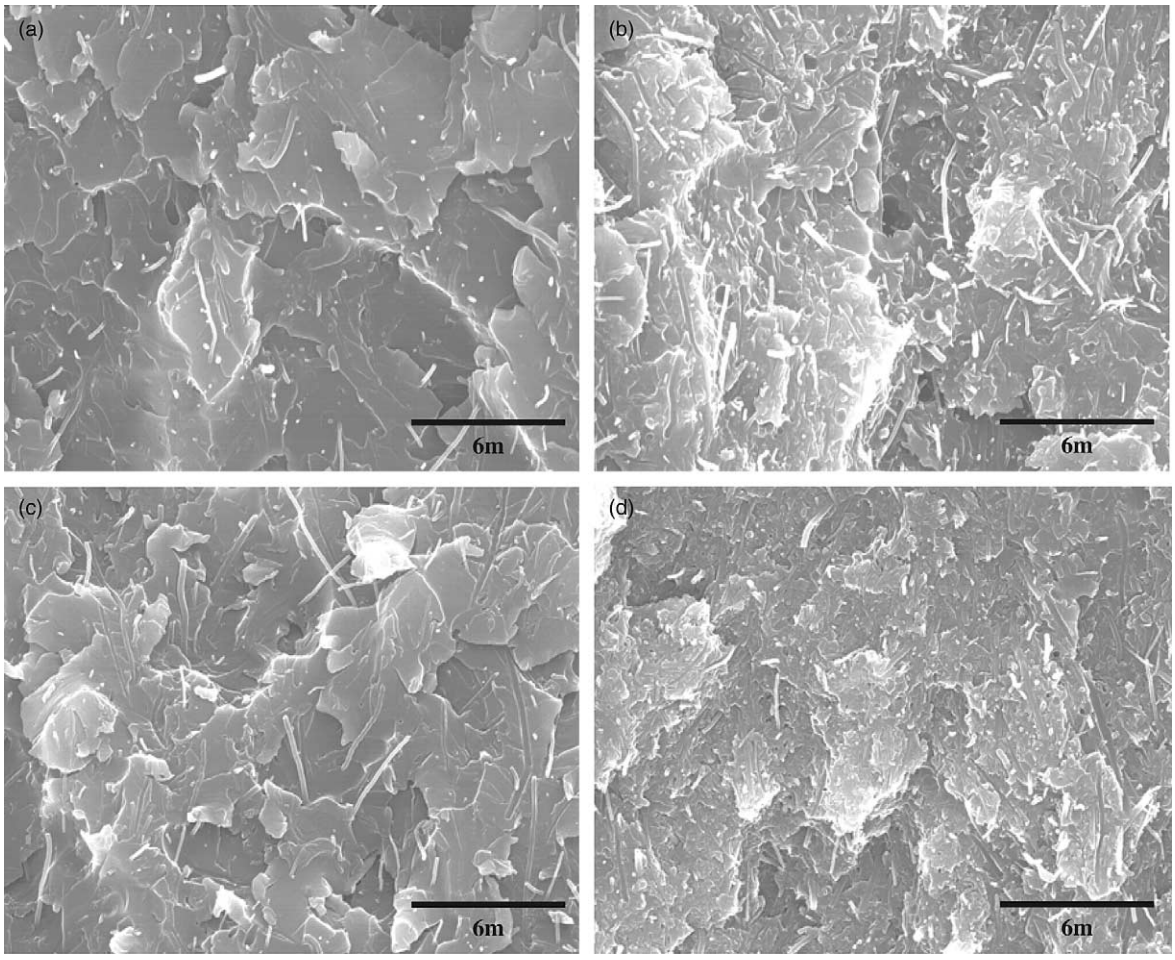


Fig. 4. SEM photography of the fracture surface of nanocomposites; (a) 5 wt% and (b) 20 wt% untreated; (c) 5 wt% and (d) 20 wt% ozone treated.

may influence the mechanical properties of the composites [39]. However, we see only one side of the composites and can not see the dispersion state of the filler in bulk by using SEM. Thus, we observed the ultramicrotome section of the composites by TEM. Fig. 5 shows the TEM images of the micortomed composites with a thickness of ca. 100 nm, which contains 5 wt% CSCNTs. From TEM observation under low magnification we found a good dispersion state of CSCNT, but the images in Fig. 5 reveals the presence of nanotubes aggregates for both untreated and treated CSCNTs in the epoxy matrix. This aggregation should affect the mechanical and electrical properties as will hereinafter be described later.

Comparing untreated and treated nanotube composites in the SEM images, we could detect the existence of more voids

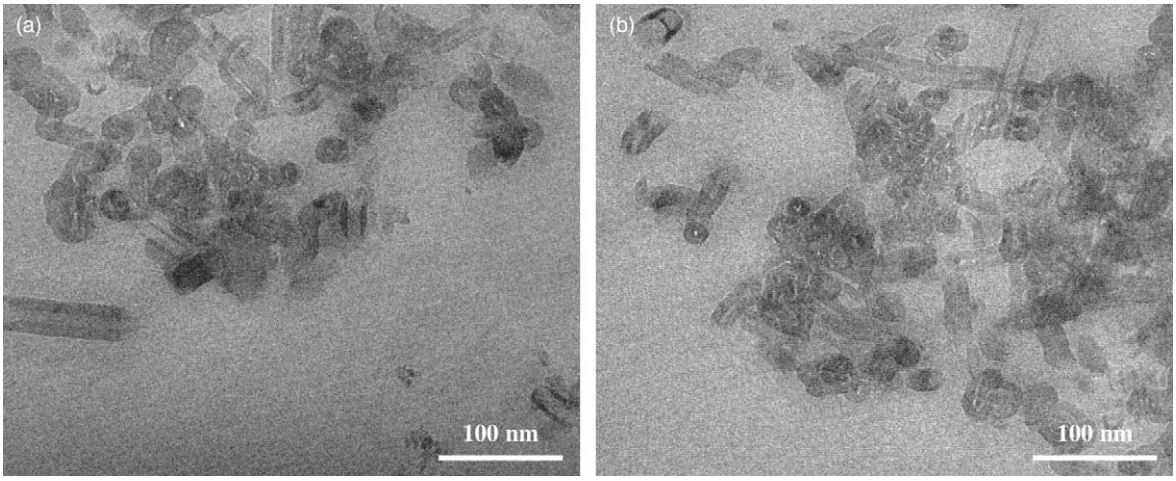


Fig. 5. TEM images of the nanocomposites; (a) 5 wt% untreated CSCNT/epoxy and (b) 5 wt% ozone treated.

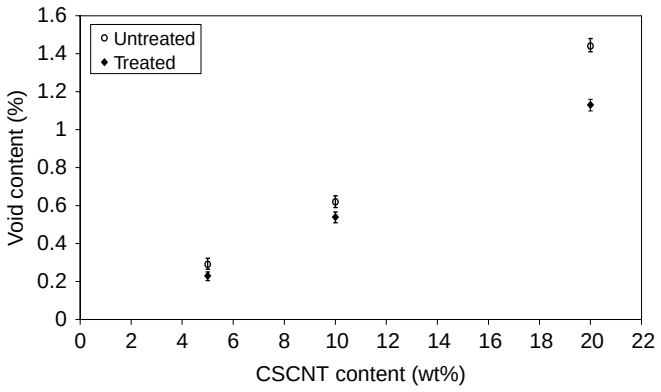


Fig. 6. Plot of the void content of nanocomposites before and after the ozone treatment of CSCNT.

in the composite including untreated CSCNT. Therefore, the void content for each composite was quantified and the results are shown in Fig. 6. As expected, the void contents increased with increasing CSCNT loading. And the void contents of the untreated composites are higher than that of treated ones. This may be attributed to the existence of voids in the interface between CSCNT and the matrix polymer due to poor wettability and the lack of ozone treatment. However, the removal of voids was not achieved even after ozone treatment, and became difficult at higher CSCNT content.

### 3.2. Surface properties of CSCNTs

The wetting behavior of the ozone treated CSCNT was characterized by contact angle using water and uncured epoxy resin. After carrying out the ozone treatment on the CSCNT surface, the CSCNT surfaces became highly hydrophilic. Table 1 reported the contact angles in epoxy resin and water on filler before and after ozone treatment. These results revealed that the epoxy and water contact angles are the lowest values for the ozone treated fillers. It is well known that the surface functional groups of fibers can play an important role in improving the surface free energy and also the adhesion between epoxy matrix and fiber. This improves the mechanical properties of the nanocomposites.

To confirm this observation, XPS measurement was performed on the CSCNTs before and after the ozone treatment. For quantification, additional results of some kinds of functional groups are given in Table 2.

As shown in Table 2, the surface oxygen concentration increased after oxygen treatment due to the introduction of oxygen onto the fiber surface. In contrast, the surface hydrogen concentration decreased from 78.47 to 76.51 at.%, which may be attributed to the replacement of oxygen. From the XPS, we analyzed the oxygen bonding and it is expected that an increase

Table 1
Contact angles on untreated and treated CSCNT

| Ozone | Water (°) | Epoxy (°) |
|---|---|---|
| Untreated | 132 | 124 |
| Treated | 52 | 103 |

Table 2
Surface oxygen functional groups in CSCNT from XPS analysis

| Ozone | C–(H,C) (at.%) | C–O (at.%) | C=O (at.%) | O–C=O (at.%) | (O–C=O)–O (at.%) | O1s/C1s ratio (%) |
|---|---|---|---|---|---|---|
| Untreated | 78.47 | 13.93 | 2.99 | 2.08 | 2.53 | 2.67 |
| Treated | 76.51 | 15.10 | 3.22 | 2.77 | 2.40 | 3.68 |

of surface functionality of the CSCNTs play an important role to improve the degree of adhesion at the interface between the fibers and the epoxy matrix.

### 3.3. Electrical properties

Fig. 7 shows the variation of electrical resistivity with CSCNT content for CSCNT/epoxy composites containing untreated and ozone-treated CSCNT. In the figure, both composite sheets are similar in terms of the electrical resistivity the CSCNT content, and show that the resistivity decreases almost linearly with an increase in fiber loading. This means that the CSCNT content made contact with other fibers and brings about an increase in the network structure for electrical conductivity with CSCNT loading. We also estimated that the electrical resistivity for the 5 wt% CSCNT is greater than that of homogeneous dispersion CNT/polymer composites of the same filler content [40]. This is due to the existence of filler aggregates in the epoxy, which were affected. However, the significant influence of the ozone treatment on the resistivity of the composites is not detected compared to the case of untreated CSCNT.

### 3.4. Mechanical properties

Fig. 8(a) and (b) shows the tensile strength and Young's modulus, respectively, for the composite with and without ozone treatment. These figures show that the reinforcement effect reaches a maximum at for tensile strength and Young's modulus at 5 wt%. A slightly higher effect of ozone treatment on the mechanical properties without treatment was expected, because the ozone treatment introduces a higher adhesive surface with epoxy resin. However, the Young's modulus results showed no significant difference for both materials and are possible due to the presence of CSCNT aggregates (Fig. 5).

The decrease in mechanical properties at higher CSCNT loading is attributed to the increase of void content, as shown in Fig. 6. As well known, the existence of defects such as voids lowers mechanical properties, especially in the case of hard and brittle materials.

However, the removal of void in the composites becomes difficult with increased filler content, because the viscosity of epoxy resin before curing is increased with CSCNT content and difficult to expel the bubbles. Therefore, some means to inhibit the formation of void will be necessary, which is now under investigation.

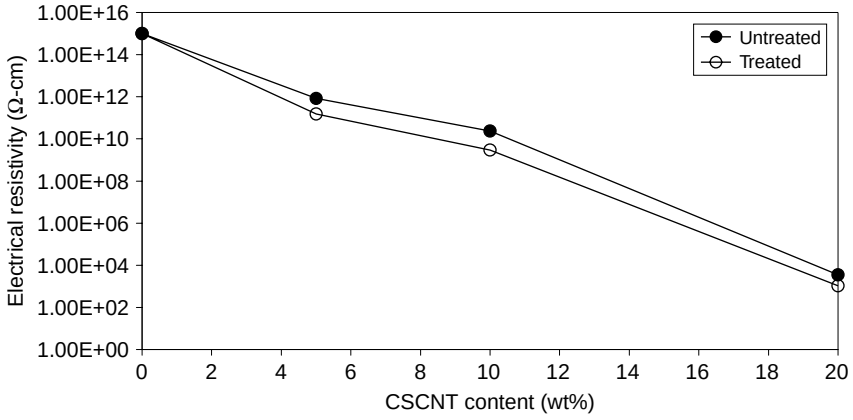


Fig. 7. Variation of electrical resistivity with CSCNT loading before and after ozone treatment.

Fig. 9(a) and (b) shows the variation of the friction coefficient of untreated and ozone-treated composites, respectively, as a function of CSCNT content. For the pure epoxy, the friction coefficient increases with an increase of load force. The friction coefficients of the composite sheets are distinctly decreased, especially at a higher load force. The lowering of the friction, i.e., better tribological property, is significantly shown at 5 wt% of CSCNT content. The friction coefficient of the ozone-treated sample is lower comparing at the same filler content for the composites with untreated CSCNT, which means a higher dispersion state of ozone-treated CSCNT in the composites. The changing trend of friction property agrees well with the results of tensile test in Fig. 8.

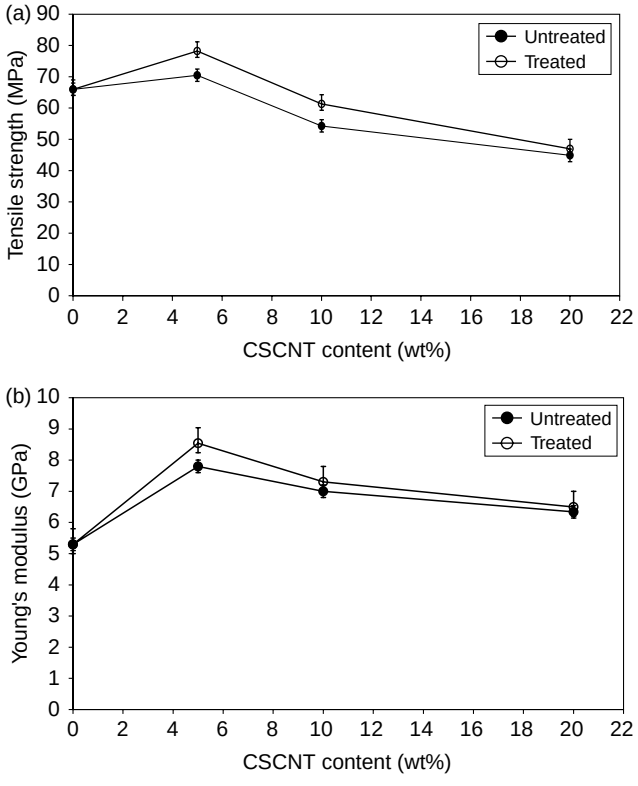


Fig. 8. Representative (a) tensile strength and (b) Young's modulus curves as a function of CSCNT loading before and after the ozone treated CSCNT nanocomposites.

Fig. 10(a) and (b) shows the variation of friction coefficients for pure epoxy and epoxy/CSCNT nanocomposites before and after the ozone treatment under various sliding speed and constant load 10 N. We estimated that the friction coefficient considerably decreased with increasing CSCNT loading at various sliding speeds. Moreover, the nanocomposites show better friction resistances at larger sliding speeds. The friction resistance of the nanocomposite becomes insensitive to the increasing content of filler when the mass fraction of CSCNT surpasses 5 wt%. This mass fraction is the same as mentioned above.

Comparing both materials, lower frictions occurred in the ozone treated fiber composite but the values for both materials were very close.

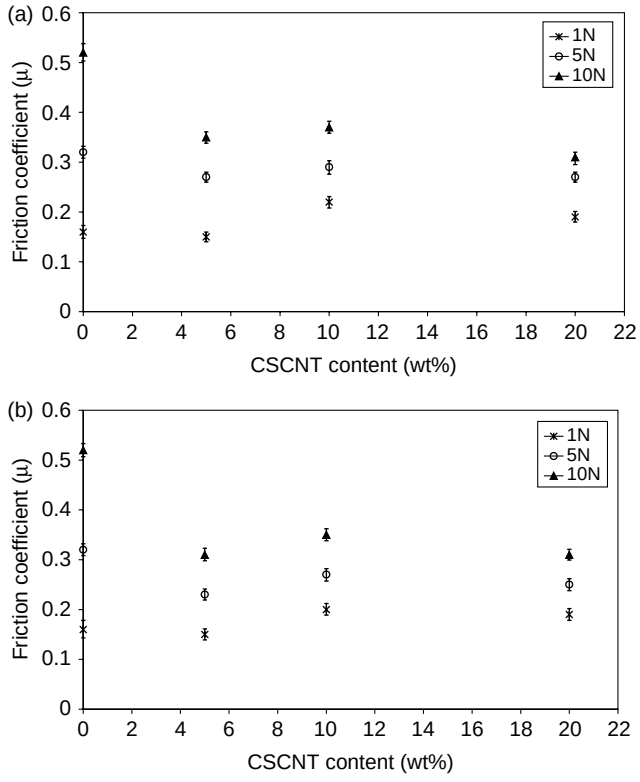


Fig. 9. Coefficient of friction as a function of CSCNT content after 50 cycles; (a) untreated and (b) treated fiber of nanocomposites.

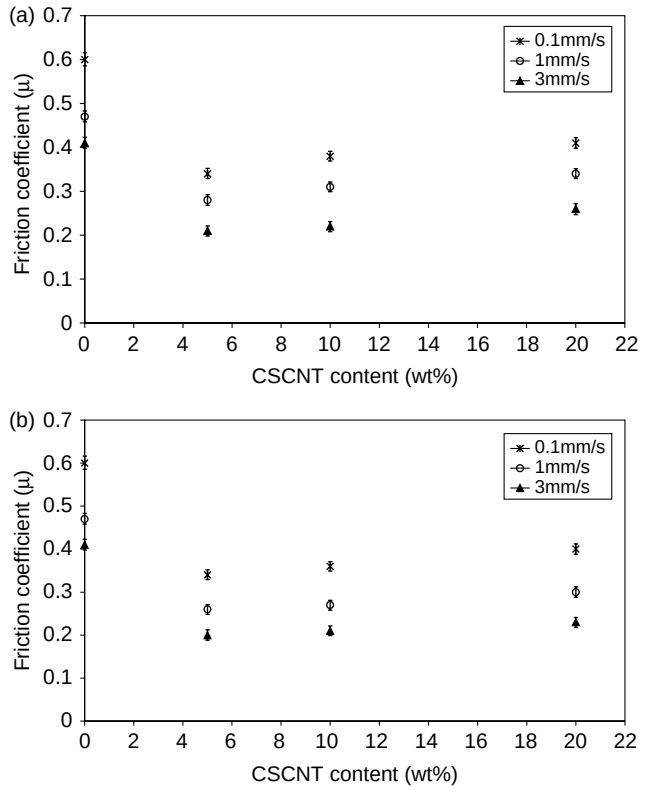


Fig. 10. Coefficient of friction as a function of CSCNT content after 20 cycles; (a) untreated and (b) treated fiber of nanocomposites.

The SEM analysis of the transfer films of pure epoxy and epoxy/ozone treated CSCNT composites under different testing conditions are shown in Figs. 11 and 12, respectively.

Fig. 11(a) shows particle detachment and debris structures along the sliding direction on the counterface under low sliding velocity. These structures correspond to the relatively poorer wear resistance to the pure epoxy. A uniform smooth surface and compact transfer film was observed in the case of epoxy/CSCNT composite, as seen in Fig. 11(b), which agrees well with the considerably decreased friction-resistance of the epoxy/CSCNT composites.

We also examined the transfer film of pure epoxy and epoxy/ozone treated CSCNT composite under large sliding velocity (Fig. 12(a) and (b)). Fig. 12 shows similar behavior as mentioned above. Comparing Figs. 11 and 12 results, it can be seen that less obvious damage appear on the transfer film under a large sliding speed as compared to that under a smaller sliding speed. It is therefore, inferred that the specimen surface becomes less damaged at a larger sliding speed.

From these results, it can be deduced that incorporation of CSCNT contributes to restrain the detachment of the epoxy matrix and improve the adhesion while decreasing the friction resistance of the CSCNT/epoxy and pure epoxy.

### 3.5. Thermal properties

Fig. 13(a) and (b) shows that the temperature dependence of $E'$ for the composites with untreated and ozone-treated CSCNT, respectively. Although the pure epoxy resin was broken around 180 °C during heating, the measurements for all composites were carried out up to 200 °C. This means higher heat resistance of the composites is enhanced by CSCNT loading. We also observed that the $E'$ values increased with an increase in fiber loading both above and particularly below $T_g$ for both composites regardless of ozone treatment. The onset of $E'$ drop corresponds to the starting of glass transition temperature of epoxy matrix, and the introduction of the fillers leads higher $T_g$ of the composites. These results shows that thermally induced molecular motion of epoxy matrix is restricted by introduced CSCNT. However, the threshold values of the filler content brings about the higher onset temperature of the $E'$ drop and is different, which are 5 wt% for ozone-treated CSCNT and 10 wt% for untreated CSCNT, respectively. $T_g$ and $E'$ above $T_g$ are increased drastically for the composite having more than 10 wt% untreated CSCNT loading. On the other hand, the lower threshold value of 5 wt% for composites with ozone-treated CSCNT is attributed to the functional groups newly introduced on the CSCNT surface by ozone treatment. That is, they react to epoxy resin, and consequently, CSCNT and epoxy resin are bound to each other

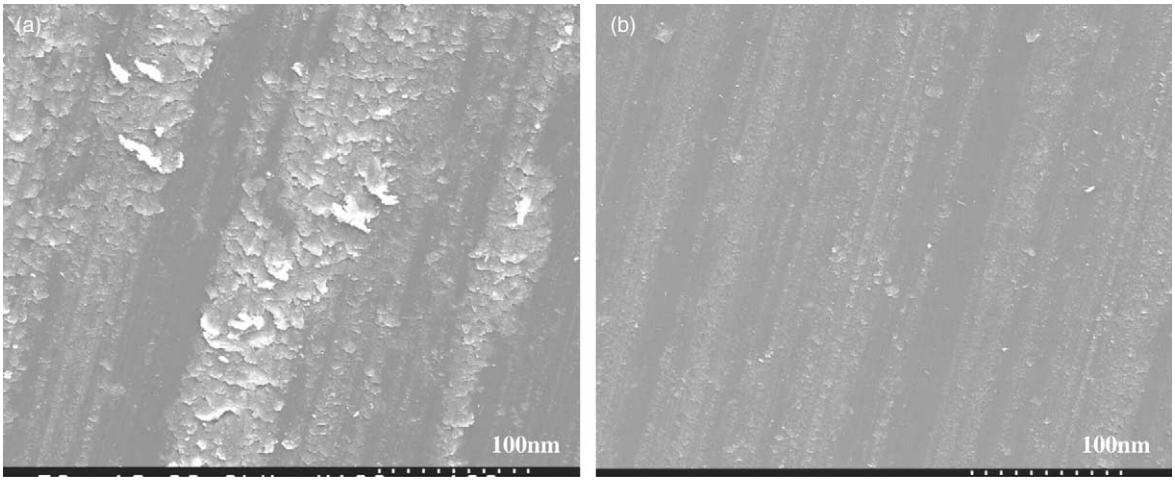


Fig. 11. SEM micrographs of (a) transfer film against pure epoxy and (b) transfer film of epoxy/5 wt% CSCNT composite (load: 10 N; sliding speed: 0.1 mm/s).

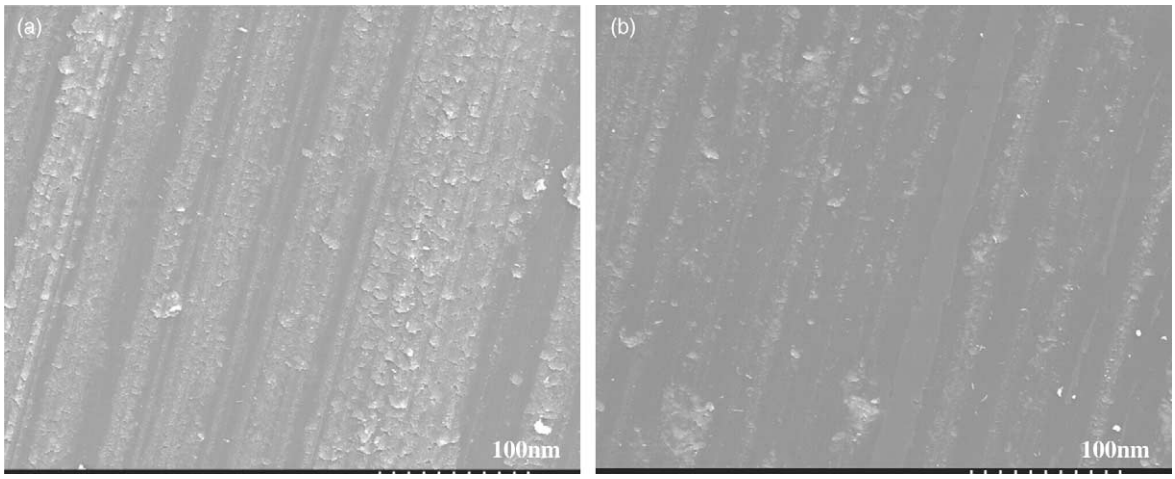


Fig. 12. SEM micrographs of (a) transfer film against pure epoxy and (b) transfer film of epoxy/5 wt% CSCNT composite (load: 10 N; sliding speed: 3 mm/s).

by covalent bonding. But the temperature of $E'$ drop for the composite including 20 wt% ozone-treated filler is observed at a lower temperature than those composites with lower filler content. The reduction of $T_g$ will be described in the next part.

Fig. 14(a) and (b) shows the temperature dependence of tan $\delta$ for the composites with untreated and ozone treated CSCNT, respectively. Prominent peaks are ascribed to the glass transition and the temperature at peak maxima exhibits the $T_g$ as defined in experimental part. For the composites having untreated CSCNT, the $T_g$ is increased and the magnitude is decreased with increased filler content. In contrast, in the case of ozone treatment, $T_g$ drastically increased, and decreased with increasing filler content. This decreasing is considered to relate to the formation of oxygen-containing functional groups on the surface of CSCNT by ozone treatment. That is, it may be caused by the adsorption of functional gropes of epoxy prepolymer or triethylenetetramine into ozone-treated CSCNT surface, as observed for the CNT composites of matrix thermosetting polymer [41,42] including epoxy resin [42]. The absorption may change the chemical equivalent between epoxy polymer

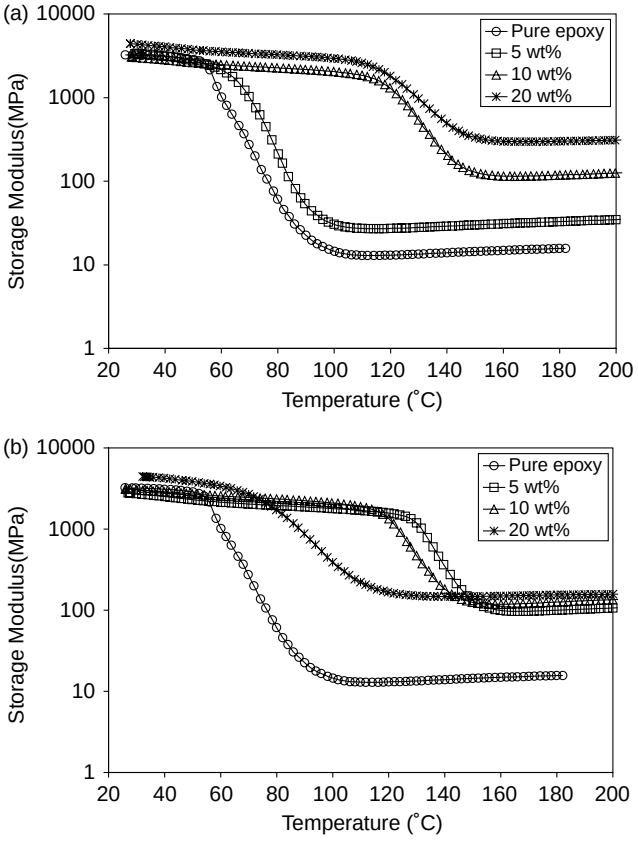


Fig. 13. Dynamic mechanical thermal analysis of epoxy nanocomposites as a function of temperature with logarithm of the storage modulus (a) ozone untreated and (b) treated fiber.

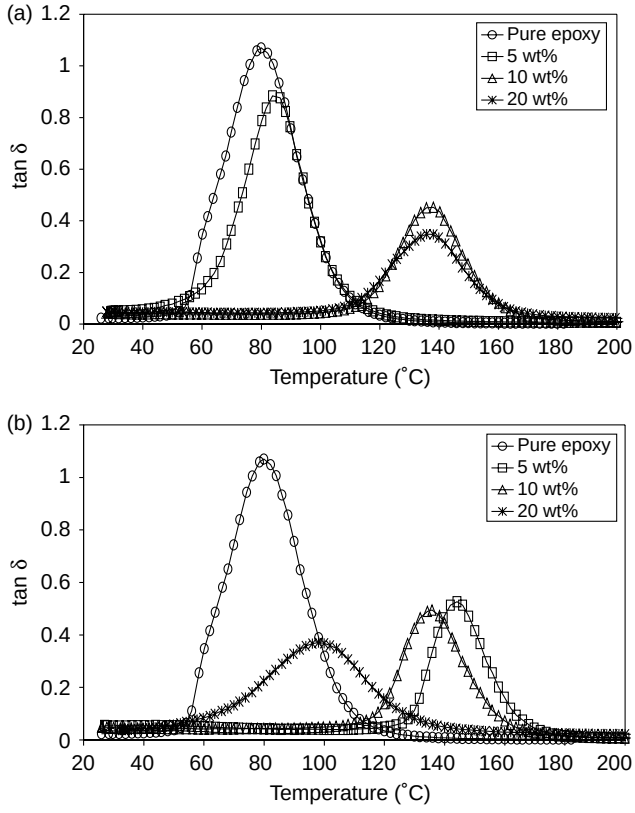


Fig. 14. Dynamic mechanical thermal analysis of epoxy nanocomposites as a function of temperature of the tan $\delta$ (a) ozone untreated and (b) treated fiber.

and triethylenetetramine, which leads to inhibition of crosslinking reaction between epoxy polymer and triethylenetetramine, which leads to an inhibition of crosslinking reation between epoxide groups and hardner. In the case that the ozone-treated fillers content is 5 wt%, the epoxide groups chemically react with the newly formed oxygen-containing groups and act as a crosslinker, and consequently the $T_g$ of the composite is increased. On the other hand, in the case that the filler content goes up to 20 wt%, the balance of the chemical equivalent between epoxy prepolymer and triethylenetetramine are altered, and the total crosslinking density in the matrix polymer may become lower. As a result, $T_g$ of the composites decreased with increased loading of CSCNT.

## 4. Conclusion

This report describes a successful route for the fabrication of nanocomposite sheets containing cup-stacked carbon nanotubes using a solution–evaporation method with a presser process. The cup-stacked CNTs were homogeneously dispersed in the epoxy matrix for both nanocomposites, but there are some aggregation in the both composites and void content increased with increasing fiber loading. The ozone treatment resulted in an increase in the form of the surface oxygen content, specifically in the form of dominant functional groups involving hydroxyl groups. The addition of CSCNT decreased the electrical resistivity for both materials. The storage modulus of the nanocomposites which significantly increased with increasing CSCNT loading fraction. Although the CSCNTs were well dispersed in the epoxy after ozone treatment but the oxygen on the surface of CSCNT broke the chains of bisphenol A. This resulted in a lower cross-link density of the epoxy resin of the CSCNT nanocomposite, which was observed from a lower glass transition temperature. Both the maximum tensile strength and Young's modulus resulted at 5 wt% for both materials. This indicates good fiber dispersion and lower void content for both 5 wt% of CSCNT composites. The coefficient of friction of both materials obtained at 5 wt% of CSCNT content was good. We estimated this was because the filler was well dispersed and had fewer voids in the nanocomposites.

## Acknowledgements

The authors like to thank Professor Nakajima Tsuyoshi of Faculty of Engineering at Shinshu University for his hospitality regarding the facilities at ozone treatment equipments and his valuable help in the useful technical discussion. The authors are grateful to Dr So Yonekubo, Precision Research Institute of Nagano Prefecture, for the XPS measurement. The authors would also thanks to Mr Asahiko Futamura for his skillful technical support toward the completion of this research work.

This work was supported by the Cluster of Ministry of Education, Culture, Sports, and Technology, Japan.

## References

[1] Dresselhaus MS, Dresselhaus G, Eklund PC. Science of fullerenes and carbon nanotubes. New York: Academic; 1996 p. 802.
[2] Treacy MMJ, Ebbesen TW, Gibson JM. Nature (London) 1996;381:678.
[3] Wong EW, Snheehan PE, Lieber CM. Science 1997;277:1971.
[4] Poncharal P, Wang ZL, Ugarte D, De Heer WA. Science 1999;283:1513.
[5] Saito R, Dresselhaus G, Dresselhaus MS. London: Imperial college press; 1998.
[6] Yakobson BI, Smalley RE. Am Sci 1997;85:324.
[7] Robertson DH, Brenner DW, Mintmire JW. Phys Rev B 1992;45:12592.
[8] Yakobson BI, Brabec CJ, Bernhole J. Phys Rev Lett 1996;76:2511.
[9] Lu JP. Phys Rev Lett 1997;79:1297.
[10] Cornwell CF, Wille LT. Solid State Commun 1997;101:555.
[11] Iijima S. Nature (London) 1991;354:56.
[12] Kamalakaran R, Terrones M, Seeger T, Kohler-Redlich P, Ruhle M, Kim YA, et al. Appl Phys Lett 2000;77(21):1.
[13] Huang ZP, Wang DZ, Wen JG, Sennett M, Gibson H, Ren ZF. Appl Phys A 2002;74(3):387.
[14] Boehm HP. Carbon 1973;11(6):583.
[15] Baird T, Fryer FR, Grant B. Carbon 1974;12:591.
[16] Oberlin A, Endo M, Koyama T. J Cryst Growth 1976;32:335.
[17] Tibbetts GG. J Cryst Growth 1984;66:632.
[18] Baker RTK, Harris PS, Terry S. Nature 1975;253:37.
[19] Endo M, Takeuchi K, Igarashi S, Kobori K, Shiraishi M, Kroto HW. J Phys Chem Solids 1993;54(12):1841.
[20] Andrews R, Jacques D, Rao AM, Derbyshire F, Qian D, Fan X, et al. Chem Phys Lett 1999;303(5-6):467.
[21] Terrones M, Grobert N, Olivares J, Zhang JP, Terrones H, Kordatos K, et al. Nature 1997;388:52.
[22] Terrones H, Hayashi T, Munoz-Navia M, Terrones M, Kim YA, Grobert N, et al. Chem Phys Lett 2001;343:241.
[23] Endo M, Kim YA, Hayashi T, Fukai Y, Oshida K, Terrones M, et al. Appl Phys Lett 2002;80(7):1267.
[24] Rinzler AG, Liu J, Dai H, Nikolaev P, Huffman CB, Rodríguez-Macías FJ, et al. Appl Phys A 1998;67(1):29.
[25] Salvetat JP, Briggs GAD, Bonard JM, Bacsa RR, Kulik AJ, Stöckli T, et al. Phys Rev Lett 1999;82(5):944.
[26] Wagner HD, Lourie O, Feldman Y, Tenne R. Appl Phys Lett 1998;72(2):188.
[27] Ajayan PM, Schadler LS, Giannaris C, Rubio A. Adv Mater 2000;12(10):750.
[28] Montes-Moran MA, Martinez-Alonso A, Tascon JMD, Paiva MC, Bernardo CA. Carbon 2001;39(7):1057.
[29] Papirer E, Donnet JB, Vidal A, Li S, Shi Z. ACS rebber division 131st meeting, Montreal; May 1987.
[30] Fu X, Lu W, Chung DDL. Cem Concr Res 1998;28(2):183.
[31] Sanchez-Polo M, Rivera-Utrilla J. Carbon 2003;41(2):303.
[32] Valdes H, Sanchez-Polo M, Rivera-Utrilla J, Zaror CA. Langmuir 2002;18:2111.
[33] Fu X, Lu W, Chung DDL. Cem Concr Res 1996;26:1007.
[34] Qian D, Dickey EC, Andrews R, Rantell T. Appl Phys Lett 2000;76:2868.
[35] Kumar S, Doshi H, Srinivasarao M, Park JO, Schiraldi DA. Polymer 2002;43:1701.
[36] Cooper CA, Ravich D, Lips D, Mayer J, Wagner HD. Compos Sci Technol 2002;62:1105.
[37] Endo M. Chem Technol 1988;18:568.
[38] Tibbetts GG, Gorkiewicz DW, Alig RL. Carbon 1993;31(5):809.
[39] Chellappa V, Chiu ZW, Jang BZ. Proc 26th Int SAMPE Tech Conf 1994;112.
[40] Breuer O, Sundararaj U. Polym Compos 2004;25(6):630.
[41] Xu J, Donohoe JP, Pittman Jr CU. Composites A 2004;35:693.
[42] Miyagawa H, Drzal LT. Polymer 2004;45:5163.